Supplementary Information (SI) for Analyst.
This journal is © The Royal Society of Chemistry 2024

Table of contents

Supplementary materials

EVs characterization: TEM, Western blot

Formvar/carbon-supported copper grids (Sigma, cat. TEM-FCF300CU50), Uranyl-less reagent (EMS, cat. 22409) were used for Transmission electron microscopy (TEM, JEOL) analysis.

11% (w/v) polyacrylamide gels (GenDEPOT, cat. a0418-050), electrophoresis buffer (Tris base 25 mM, glycine 250 mM, 1% SDS dissolved in deionized water and adjusted to pH 8.3 using NaOH and HCl), transfer buffer (Tris base 25 mM, glycine 192 mM dissolved in deionized water and adjusted to pH 8.3 using NaOH and HCl), primary antibodies (CD81: 1.3.3.22 clone, SCBT, SC7367; CD9: MEM61 clone, SCBT, cat. SC51575; CD63: NK1C3 clone, SCBT, cat. SC59286), HRP-conjugated secondary antibodies (anti-mouse HRP; bio Rad, cat. 170-6516), chemiluminescent substrates (Amersham, cat. RPN2232) was used for western blotting.

Aggregation analysis

CD81: 5A6 clone (SCBT, cat. SC23962); 1.3.3.22 clone (SCBT, cat. SC7367), CD9: (SCBT, cat. SC51575, and Biolegend, cat. 312102), and CD63 (SCBT, cat. SC59286 and Biolegend, cat. 353039) antibodies and secondary antibodies (Anti-rabbit secondary antibody conjugated with HRP (SCBT, cat. SC2004), anti-mouse AF488 secondary antibody (Invitrogen, cat. A21131)) were used.

Supplementary methods

Cell culture

HEK293T cells were cultured in high-glucose Dulbecco's Modified Eagle Medium (DMEM, Gibco, 12100046) supplemented with 10% Fetal Bovine Serum (FBS, Gibco, 12483020) and 1% antibiotic-antimycotic (Anti-anti, Gibco, 15 240 062) in a 37°C, 5% CO_2 humidified incubator. Cells were split into a 5 to 1 ratio when they were ~90% confluent.

Zeta potential measurement of Extracellular vesicles using Dynamic light scattering (DLS)

Zeta potential was measured using Dynamic light scattering (Malvern instruments, cat. Zetasizer 3000HSA). The measurements were carried out in a folded capillary cell (cat. DTS1070). The concentration of EVs was adjusted to achieve count rates (kcps) between 50 and 500 by diluting them with filtered PBS. The instrument was operated in an auto mode for each set of buffer conditions.

Statistical analysis

Two-tailed unpaired Welch's t-tests were conducted using GraphPad Prism 5 software and Microsoft Excel, and the data were presented as mean ± standard deviation (SD). Numbers of technical replicates are indicated as 'n', and biological replicates are indicated as 'N'. Pairs showing p-value smaller than 0.05 were considered statistically significantly different and depicted with a star (*, $p < 0.05$) and (**, $p < 0.01$).

Supplementary Description

Calculation of actual number of particles in homo-aggregates and hetero-aggregates for aggregation ratio (%)

The probabilities of homo-aggregates and hetero-aggregates are respectively

$$\frac{1}{2^{(k-1)}} \text{ and } \left(1-\frac{1}{2^{(k-1)}}\right)$$

When N represents the actual total number of particles, the total cases of homo-aggregates and hetero-aggregates are respectively

$$N_{homo,k} = N \times \left(\frac{1}{2^{(k-1)}}\right)$$

$$N_{hetero,k} = N \times \left(1 - \frac{1}{2^{(k-1)}}\right)$$

Supplementary Table1. Detailed values and example calculations for Aggregation index

Detection	Green (pts)	Red (pts)	Colocalized (=Nhetero) (pts)	Total (pts)
Before aggregation	$n_{g,1}$	$n_{r,1}$	$n_{gr,1}$	$n_{g,1}+n_{r,1}-n_{gr,1}$
After aggregation	$n_{g,2}$	$n_{r,1}$	$n_{gr,2}$	$n_{g,2}+n_{r,2}-n_{gr,2}$

Analysis	Colocalization	Ratio (%)	Aggregation ratio (A_k(2))	Ratio (Real case) (%)
Before aggregation	$n_{gr,1} / Total_1$	8.0%	$(n_{gr,1} + n_{homo,1}) / Total_1$	16.0%
After aggregation	$n_{gr,2} / Total_2$	28.4%	$(n_{gr,2} + n_{homo,2}) / Total_2$	56.8%

Sample	Ngreen	Nred	Nhetero	Ntotal	Colocalization (%)	Aggregation ratio (%)
Detected value #1	27	258	217	448	6.00%	12.10%
Detected value #2	26	285	153	412	6.30%	12.60%
Detected value #3	28	261	182	415	6.70%	13.50%
Detected value #4	48	284	211	447	10.70%	21.50%
Detected value #5	56	298	197	439	12.80%	25.50%

Supplementary Figures

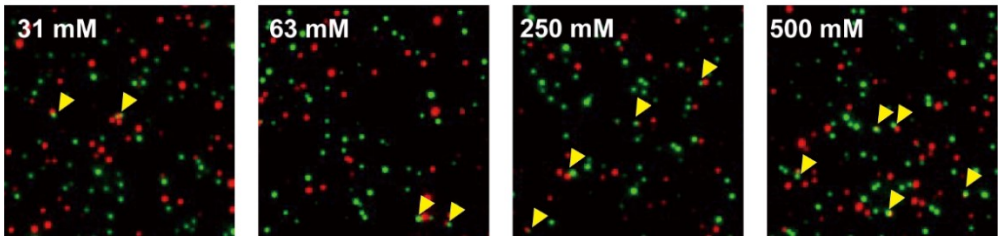

Supplementary Figure 1. Images of EV aggregation in salt concentration Observation of EV aggregation in TIRFm images as increasing salt concentration. From left to right: 0.25x (31 mM), 0.5x (63 mM), 2x (250 mM), and 4x (500 mM) based on salt concentration in 1x PBS.

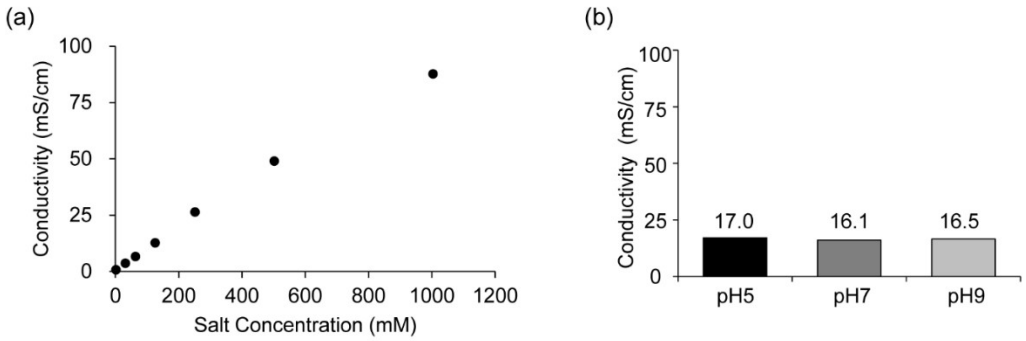

Supplementary Figure 2. Conductivity of salt concentration and pH variation of buffer (a) Increase in conductivity with increasing salt concentration. (b) Conductivity with pH change.

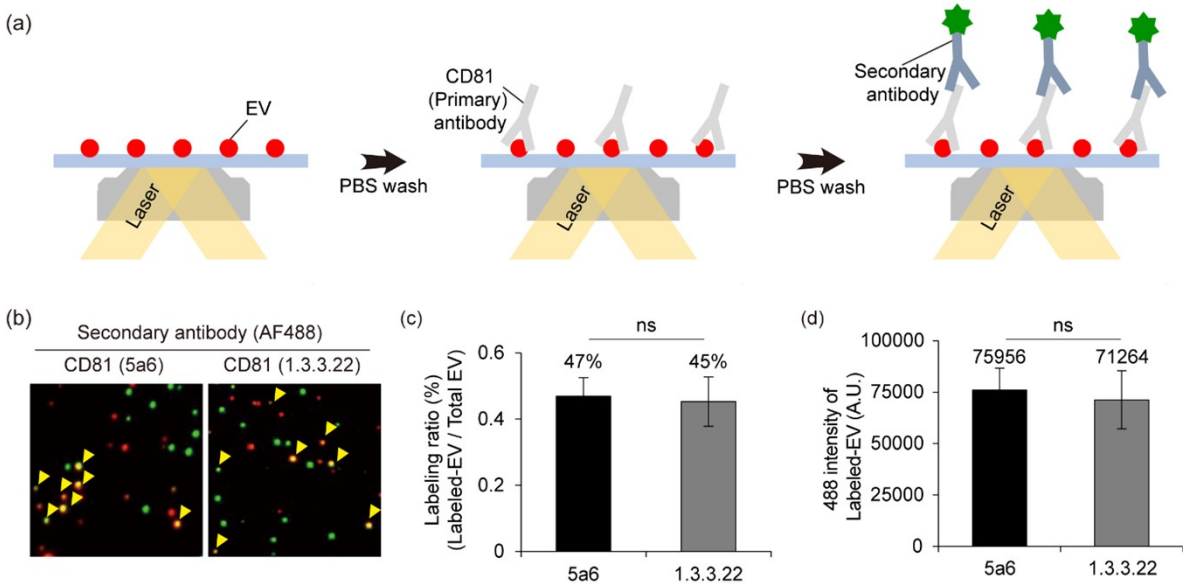

Supplementary Figure 3. Characteristics of antibody promoting EV aggregation (a) Schematic of labeling efficiency and fluorescence intensity for different CD81 antibody (5a6 and 1.3.3.22) clones (b) Images of EV (red) stained with different CD81 antibodies (5a6 and 1.3.3.22) clones using a secondary antibody (green) (c) The ratio of EVs labeled with CD81 antibody to the total EVs (Bars: mean ±SD, N>9, two-tailed unpaired Welch's t-

test was performed.) (d) The 488 fluorescence intensity of CD81-stained EVs. (Bars: mean ± SD, n=4, two-tailed unpaired Welch's t-test was performed, *p<0.05). (Black: 5a6, Gray: 1.3.3.22, clone)

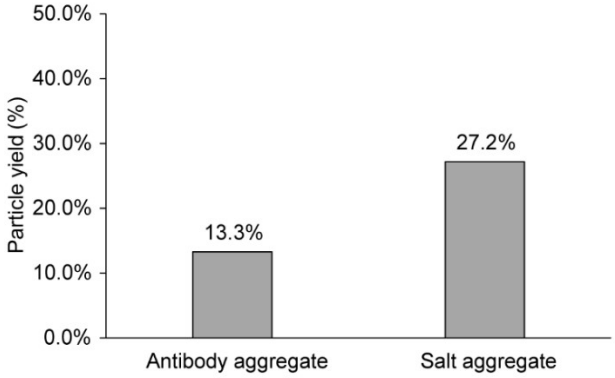

Supplementary Figure 4. Particle yield for removal methods with high salt- and antibody(5a6) -aggregates
Quantification of particle yield before and after passage through a PCTE filter with 200 nm pores using Nanoparticle Tracking Analysis for two types of aggregates.